Breathing Pattern Detection Using a Graphite-Based Paper Sensor for Development of an Auto-Calibrating CPAP System

Submitted in partial fulfilment of the requirement for the award of the degree of

Bachelor of Technology

in

Applied Electronics & Instrumentation Engineering

By:

Name	**University Reg. No**	**University Roll No**
Anjan Mahuri	221260110006 (2022–26)	12622005006
Raunak Das	221260110033 (2022–26)	12622005033
Sagnik Das	221260110037 (2022–26)	12622005037
Sarthak Sardar	221260110039 (2022–26)	12622005039

Under the Supervision of

Prof. (Dr.) Madhurima Chattopadhyay

Head of the Department

Department of Applied Electronics & Instrumentation Engineering
Heritage Institute of Technology, Kolkata

DEPARTMENT

OF

APPLIED ELECTRONICS INSTRUMENTATION ENGINEERING

HERITAGE INSTITUTE OF TECHNOLOGY

CERTIFICATE

This is to certify that the project work entitled

"Breathing Pattern Detection Using a Graphite-Based Paper Sensor for Development of an Auto-Calibrating CPAP System"

has been successfully completed by:

Name	**University Reg. No**	**University Roll No**
Anjan Mahuri	221260110006 (2022–26)	12622005006
Raunak Das	221260110033 (2022–26)	12622005033
Sagnik Das	221260110037 (2022–26)	12622005037
Sarthak Sardar	221260110039 (2022–26)	12622005039

In partial fulfilment of the degree of

Bachelor of Technology
in
Applied Electronics & Instrumentation Engineering
Maulana Abul Kalam Azad University of Technology, 2025

Name of the project guide: Prof. (Dr.) Madhurima Chattopadhyay

centring Project Guide

centring External Examiner

Dept. of AEIE

Prof. (Dr.) Madhurima Chattopadhyay
Head of the Dept.
Dept. of AEIE

CONTENTS

I INTRODUCTION ii
- I-A Types of Humidity Sensing Techniques ii
- I-B Limitations of Conventional Humidity Sensors ii
- I-C Traditional Versus Sustainable Approaches to Humidity Sensing iii
- I-D Sustainable Development Goals and Bio-Eco Friendly Sensor Technologies iii

II Paper as an alternate medium iv

III Electrode Selection iv

IV Development and experimental testing of paper sensor iv
- IV-A Sensor Devlopment iv
- IV-B Heat Pad Fabrication vii

V Calibration Calculations vii
- V-A Voltage Divider Principle vii
- V-B Example Calculation vii
- V-C Method of Graph Plotting vii

VI Component List and Experimental Setup and Process viii
- VI-A Controlled Humidity Chamber viii
- VI-B Sensor Placement viii
- VI-C Fan Control Logic viii
- VI-D Data Acquisition and Analysis viii
- VI-E Component List viii

VII Results viii
- VII-A Analysis of Sensor Response Graphs ix
  - VII-A1 Humidity Response ix
  - VII-A2 Electrode Trace Degradation Rate ix
  - VII-A3 Operational Cycles x
  - VII-A4 Sensitivity to Small Humidity Changes x
  - VII-A5 Resistance Increase Mechanism x
- VII-B Performance of the Polypropylene Cloth Sensor x
  - VII-B1 Humidity Response x
  - VII-B2 Flexibility and Mechanical Stability xi
  - VII-B3 Longevity and Degradation xi
  - VII-B4 Stability of Electrical Response xi
  - VII-B5 Overall Behaviour xii
- VII-C Summary of Challenges and Outlook xii

VIII Future Prospects xiii
- VIII-A CPAP - continuous positive airway pressure xiii
- VIII-B Tank to Mask Miniaturisation xiv

IX Conclusion xiv

References xiv

Abstract

This work presents the development and preliminary optimisation of a paper-based humidity sensor intended for integration into a breathing rate detection system capable of autoregulating continuous positive airway pressure therapy. Building on sustainable sensor design principles, the study evaluates multiple paper and cloth substrates treated with graphite and sodium chloride to identify an architecture that exhibits stable ionic and electronic conduction under rapid humidity transients associated with respiratory flow. A controlled tank-based humidity cycling system was constructed to simulate inhalation and exhalation conditions allowing detailed comparison of sensor sensitivity, response time drift and structural degradation across substrates. The results demonstrate that substrate morphology and graphite stability critically influence the fidelity of humidity driven resistance modulation thereby guiding the selection of an optimized sensor design for real time respiratory monitoring. The next phase of the project will embed the characterized sensor into a nebulizer mask where breathing induced humidity oscillations can be quantitatively captured and used to control CPAP pressure delivery. This study establishes the feasibility of a low cost biodegradable humidity sensor for respiratory diagnostics while outlining its pathway toward closed loop CPAP automation.

Index Terms

Paper-based humidity sensor, biodegradable sensors, respiratory monitoring, CPAP autoregulation, graphite-NaCl conductive substrate

I. INTRODUCTION

Humidity monitoring is essential in a broad range of industrial and environmental applications, spanning manufacturing, storage, agriculture, indoor air quality management, and more. Accurate and reliable humidity measurements are critical to ensuring product quality, optimising operational efficiency, and safeguarding environmental health. Recent advancements in sensor technology have diversified the landscape of humidity sensing devices, offering solutions tailored to varied performance needs and cost constraints.

A. Types of Humidity Sensing Techniques

Humidity sensing technologies have become indispensable across diverse sectors such as agriculture, healthcare, heating, ventilation and air conditioning (HVAC) systems, environmental monitoring, and industrial automation. The selection of a humidity sensor depends heavily on the specific application's requirements, including accuracy, response time, durability, cost, and environmental conditions. The primary categories of humidity sensors, each with unique working principles, strengths, and limitations, are detailed below:

- **Capacitive Humidity Sensors:** These sensors operate by measuring the change in the dielectric constant of a hygroscopic polymer or metal oxide layer as it absorbs water vapor [1]. Typically comprising two metal electrodes separated by the sensing layer, the absorbed moisture alters the capacitance, which is then translated into humidity readings. Capacitive sensors dominate the market due to high accuracy (often ± 2–3% RH), long-term stability, wide humidity range (0–100% RH), and relatively low power consumption. They are widely deployed in industrial, commercial, and IoT applications. However, capacitive sensors are sensitive to temperature fluctuations, require periodic calibration, and may experience degradation when exposed continually to harsh moisture conditions. Their output is generally linear, and modern sensors feature integrated temperature compensation to improve accuracy [2].
- **Resistive (Conductive) Humidity Sensors:** Resistive sensors rely on detecting changes in the electrical resistance of a hygroscopic medium, typically composed of polymer films, conductive salts, or ceramics, as moisture content varies [2]. The absorption or desorption of water vapor alters ionic or electronic conduction pathways, resulting in resistance variation. These sensors are cost-effective and suitable for low-end consumer applications but often display non-linear responses, are prone to contamination and aging effects, and have limited operational temperature ranges (commonly from $-40°$C to $100°$C). Their response times range from a few seconds to tens of seconds, and they often require frequent recalibration [1].
- **Thermal Conductivity Sensors:** Based on measuring differences in thermal conductivity between dry air and humid air, these sensors typically contain two thermal elements—one sealed in dry nitrogen and another exposed to ambient air. The difference in heat transfer rates correlates with absolute humidity [3]. Thermal sensors excel in high-humidity environments and specific laboratory measurements that require absolute humidity data. However, their disadvantages include bulky size, high power consumption, slower response times, and comparatively higher cost [4].
- **Optical Humidity Sensors:** These sensors exploit changes in optical properties—such as light absorption, reflection, or scattering—caused by humidity-sensitive materials [5]. While optical sensors provide high precision and fast response times with immunity to electromagnetic interference, their complexity and cost limit their widespread adoption. Furthermore, they are generally unsuitable for harsh or dusty environments due to sensitivity to particulates and mechanical fragility [1].

Each humidity sensing technique presents inherent trade-offs. Capacitive sensors are preferred for their wide applicability and robustness in commercial and industrial domains but still face challenges in harsh or variable environments. Resistive sensors offer simplicity and cost benefits but compromise on linearity and longevity. Thermal and optical types cater to niche applications demanding specific absolute humidity data or high precision but are often impractical for large-scale or low-power deployments [2], [3], [5].

Ongoing advancements in materials and sensor design aim to mitigate these conventional drawbacks by enhancing sensitivity, stability, power efficiency, and environmental friendliness, driving the evolution of next-generation humidity sensing technologies [4].

B. Limitations of Conventional Humidity Sensors

Despite their widespread adoption, conventional humidity sensors face several notable limitations that impact performance, cost, and environmental sustainability. First, the high manufacturing costs of these sensors primarily arise from the reliance on expensive and sometimes scarce materials, as well as intricate fabrication techniques requiring sophisticated equipment and multi-step processes [6]–[8]. This economic factor restricts their large-scale deployment, particularly in resource-constrained environments.

Environmental concerns are increasingly significant, as many traditional sensors incorporate non-biodegradable and toxic components such as certain polymers, metals, and ceramics, thus contributing to the growing issue of electronic waste (e-waste).

The disposal and degradation of these sensors can lead to the release of harmful substances, posing risks to ecosystems and public health [9], [10].

The rigid and bulky form factors characteristic of many conventional sensors present integration challenges in emerging areas such as flexible electronics and wearable health monitoring devices. This mechanical inflexibility limits their utility in applications demanding conformability, light weight, and biocompatibility [9], [10].

Power consumption remains a critical drawback, especially for thermal conductivity and optical humidity sensors. These sensor types generally require higher energy input due to heating elements or complex optical detection systems, rendering them less suitable for battery-powered, portable, or IoT applications where energy efficiency is paramount [1], [6].

Long-term stability also poses challenges. Sensor drift caused by contamination, material aging, or hysteresis effects leads to degradation of accuracy and repeatability over time [1]. For example, polymer-based sensing membranes may suffer swelling, solubility issues, or reduced sensitivity in fluctuating humidity or temperature conditions. Frequent calibration and maintenance are often mandatory to mitigate these effects, raising operational costs and limiting sensor lifespan [1], [8].

Temperature dependence further complicates the measurement accuracy of several common sensor types, necessitating temperature compensation or dual-sensor systems, thereby adding complexity and cost [6].

Moreover, many resistive and capacitive sensors display limited sensitivity at very low humidity ranges, below approximately 20–30% RH, restricting their effectiveness in arid environments or specialized industrial processes [1], [6].

In summary, while conventional humidity sensors have proved invaluable in numerous applications, their limitations in cost, environmental impact, mechanical adaptability, power consumption, and long-term reliability motivate ongoing research towards new materials, designs, and fabrication methods aimed at producing more sustainable, flexible, and robust humidity sensing solutions [6], [9], [10].

C. Traditional Versus Sustainable Approaches to Humidity Sensing

Industry-standard sensors such as the DHT series (e.g., DHT11 and DHT22) exemplify traditional solutions favored for affordability, simplicity, and ease of use across home automation, educational, and small-scale environmental monitoring applications [11], [12]. However, these sensors' limitations in accuracy, durability, and response speed restrict their application in rigorous industrial and environmental contexts [13].

In contrast, emerging lab-fabricated paper-based sensors represent a sustainable alternative, leveraging biodegradable, flexible materials aligned with eco-friendly technological trends. Advances in material science have enhanced the sensitivity and reliability of paper-based sensors, situating them as promising candidates in cost-sensitive and sustainability-conscious use cases [9], [10].

This study undertakes a comparative performance evaluation between the established DHT11 sensor and lab-fabricated paper-based graphene humidity sensors. Through analysis of accuracy, response time, durability, and cost-effectiveness, the research aims to replicate DHT11 capabilities within a paper sensor framework. The outcomes will provide insight into the feasibility of sustainable sensor technologies in industrial and environmental humidity monitoring, balancing performance with eco-conscious design [9], [10].

D. Sustainable Development Goals and Bio-Eco Friendly Sensor Technologies

The development and deployment of humidity sensors play an integral role in achieving several United Nations Sustainable Development Goals (SDGs), particularly those related to environmental sustainability, health, and responsible resource management. The SDGs emphasize economic growth, social inclusion, and environmental protection—pillars that align closely with the adoption of bio-eco-friendly sensor technologies in environmental monitoring [9], [10].

Paper-based sensors epitomize sustainable innovation by leveraging biodegradable, flexible materials that reduce reliance on non-renewable resources and mitigate electronic waste problems associated with traditional sensors. This eco-friendly approach supports SDG 12 (Responsible Consumption and Production) by minimising hazardous materials and waste during sensor fabrication and disposal. Furthermore, the reduced energy consumption and carbon footprint of such sensors cater directly to SDG 13 (Climate Action), advancing efforts to combat climate change through sustainable technology [9].

These sensors also contribute to SDG 6 (Clean Water and Sanitation) and SDG 15 (Life on Land) by enabling widespread, affordable environmental monitoring that can detect pollutants and changes in humidity crucial for ecosystem health. The portability, low cost, and ease of deployment allow for large-scale screening and real-time data collection, empowering communities and authorities to make informed decisions that protect water quality, soil health, and biodiversity [10].

Biosensors such as paper-based graphene sensors exemplify the transition towards sustainable IoT-enabled environmental monitoring frameworks, promoting cleaner technologies, reducing toxic chemical usage, and supporting remote and continuous sensing applications. Their integration facilitates progress in achieving multiple SDGs by promoting responsible consumption, reducing waste and energy use, and enabling better ecosystem management [9], [10].

By prioritising these bio-eco-friendly sensor technologies, research and industry can align technological innovation with global sustainability targets, paving the way for greener, smarter, and more resilient environmental monitoring solutions [9], [10].

II. Paper as an alternate medium

Paper, due to its biodegradability, abundance, and low cost, presents an ideal substrate for environmentally sustainable sensor technology [14], [15]. Utilizing paper substrates significantly reduces reliance on non-renewable resources [14]. Additionally, the manufacturing process is simple. Using common materials like pencils and copper tape eliminates the need for complex, energy-intensive industrial processes, making production both facile and cost-effective [16].

The choice of paper type is crucial before sensor fabrication since substrate properties directly influence device performance [14]. Various types of paper have been compared for electrode fabrication, including filter paper, vegetable parchment, office paper, photo paper, and chromatography paper [16], [17]. Whatman Grade 1 filter paper is widely recognized as a robust substrate choice for sensors due to its consistency, purity, and physical properties. With medium retention (11 μm) and flow rate, Whatman Grade 1 is suited for applications that demand both mechanical stability and accessibility for electrode fabrication [18]. Its composition of high-quality alpha-cellulose ensures minimal impurities and high wet strength, which is valuable in sensor construction where durability and uniformity are critical [14].

Due to these properties, Whatman Grade 1 is frequently chosen for fabricating electrodes and as a versatile substrate in paper-based sensors, especially when reliable performance and simple processing are priorities [16].

Guided by this evidence, sensor development and testing in this work focused on two types of paper substrates.

III. Electrode Selection

In this study, electrodes were fabricated using 10B-grade graphite pencils directly on paper substrates due to their ease of use, low cost, and accessibility [19]–[21]. The high graphite content in 10B pencils provides sufficient conductivity for sensor operation, with initial resistances ranging from 40 kΩ to 70 kΩ, which is suitable for integration with voltage divider circuits and analog-to-digital conversion systems [19], [21].

Graphite pencil electrodes offer a straightforward method for rapid prototyping, as no complex equipment or specialized materials are required [20]. However, experimental results revealed challenges related to electrode durability. The graphite traces degrade over time, mainly due to moisture absorption and physical wear during repeated humidity cycles [21]. This degradation is evident from significant increases in resistance, sometimes exceeding 1 MΩ, leading to signal inaccuracies and sensor failure [20], [21].

While the use of graphite pencils enables functional sensor prototypes, limitations in long-term stability indicate that alternative electrode materials such as metallic or graphene inks may improve performance [22]–[24]. These alternatives provide enhanced conductivity, better adhesion, and greater resistance to moisture-induced degradation, which can extend sensor lifespan and reliability in demanding applications [22], [23].

Therefore, the electrode choice reflects a balance between fabrication simplicity and sensor durability. Graphite pencils serve well for initial testing and exploration, but more advanced materials are recommended for future development to address stability concerns [20], [22]–[24].

IV. Development and experimental testing of paper sensor

In this section, we have fabricated the sensor, and the detailed fabrication technique is described.

A. Sensor Devlopment

- **Material selection:**

Grade A filter paper, with a thickness ranging from 0.17 mm to 0.93 mm, was selected as the substrate for the flex sensor due to its lightweight, flexible, and porous structure. A 10B high-quality graphite pencil was used to coat the paper evenly, forming a conductive electrode. The thin copper tape was applied to both edges of the sensor, serving as a probe to facilitate electrical connections. Additionally, distilled water and sodium chloride (NaCl), commonly available as table salt, were employed during the fabrication process to enhance conductivity.

- **Chemical Properties**

The chemical properties of graphite and sodium chloride (NaCl) are integral to the sensor's enhanced performance:

(a) Graphite: Graphite, a crystalline form of carbon, is characterized by its excellent electrical conductivity, approximately 3×10^3 S/m. Its honeycomb-like layered structure consists of hexagonally arranged carbon atoms, where delocalized electrons move freely between layers, enabling efficient electrical conduction. This layered structure also imparts flexibility, making graphite suitable for applications requiring mechanical deformation, such as flex sensors [25], [26], [27], [28].

(b) Sodium Chloride (NaCl): When dissolved in distilled water, NaCl dissociates into sodium (Na^+) and chloride (Cl^-) ions, as represented by the dissociation equation:

$$\mathrm{NaCl\ (s)} \xrightarrow{\mathrm{H_2O}} \mathrm{Na^+(aq)} + \mathrm{Cl^-(aq)}$$

These ions enhance the sensor's conductivity through ionic conduction, which complements the electronic conduction provided by graphite. This synergistic effect significantly improves the sensor's sensitivity and performance.

This process generates sodium (Na^{+}) and chloride (Cl^{-}) ions, enhancing the graphite-coated paper's electrical conductivity. These ions stabilise the electrical pathways, improving the sensor's sensitivity and responsiveness to mechanical deformations. The combination of graphite's conductive, layered structure and NaCl's ionic dissociation significantly enhances the sensor's overall performance across various applications [29].

- **Geometry selection:**

Then the outline structure of the sensor is drawn on the filter paper and the area is filled by the pencil graphite as shown in fig.1

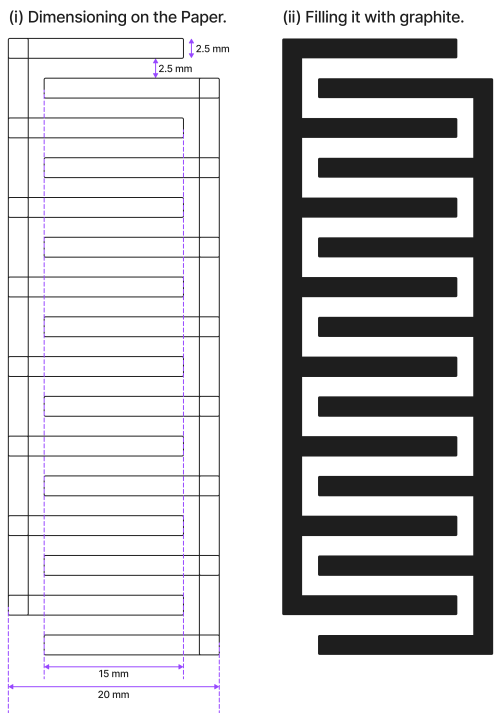

Fig. 1: Geometric dimensions of the sensor

- **Sensor fabrication:**

The sensor fabrication process begins by first outlining the sensor on a white filter paper, as shown in Fig.1. Step (i), Creating precise straight lines using a ruler as per the specified measurements: a total width of 20 mm, an internal pathway width of 2.5 mm, and a 2.5 mm gap between adjacent paths. This step ensured uniformity and accuracy in the interdigitated pattern. Once the outline is complete, the next step (ii) involves filling the designated area with graphite using a 10B graphite pencil. This step is crucial to creating a consistent, even layer of graphite, which serves as the primary conductive element of the sensor.

Step (iii) after applying the graphite layer, a layer of sodium chloride (NaCl) solution is applied using a dropper on the surface of the sensor where graphite is deposited, ensuring complete coverage as shown in Fig.5. This solution was prepared by dissolving 1 gram of common kitchen salt (NaCl) in 5 ml of distilled water (H_2O), achieving a solubility ratio of 1g/5ml. Then the paper is left to dry overnight under normal room conditions. This step enhances the electrical conductivity of the graphite by introducing ions from the NaCl solution, which improves the sensor's sensitivity.

Once the paper is completely dry, copper tape is placed on both sides of the graphite-coated area to act as electrical probes, as shown in fig.**??** and step (iv).

In the final stage of fabrication (step (v)), two wires are soldered to the copper tape at each end of the sensor. These wires provide the necessary electrical connections, allowing the sensor to be integrated into external circuits for testing and use, as shown in Fig.**??**.

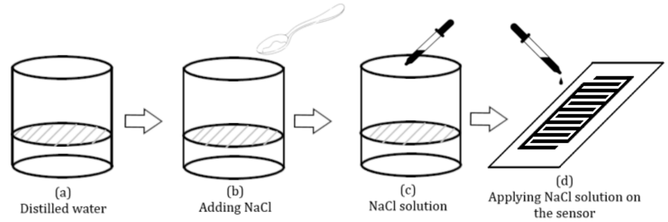

Fig. 2: Step (iii) (a-d) Schematic demonstration of NaCl solution preparation and application on the sensor.

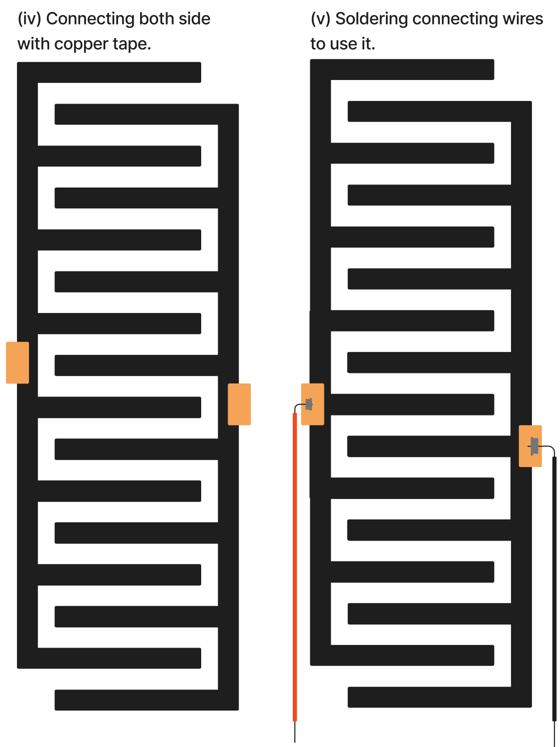

Fig. 3: The completely developed paper sensors.

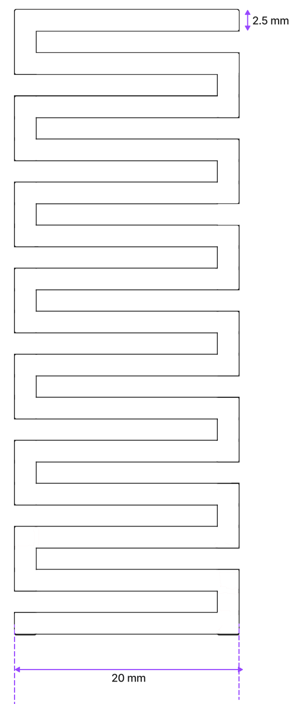

Fig. 4: The developed heatpad.

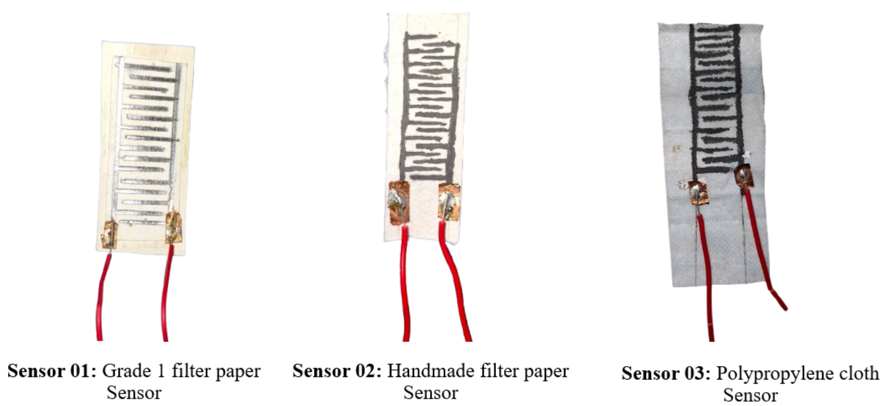

Fig. 5: The 3 types of sensors that were developed and analyzed for optimization

B. Heat Pad Fabrication

The heat pad used to maintain sensor dryness is fabricated from aluminium foil arranged in a serpentine pattern, as illustrated in Figure 4 [30]. When a voltage is applied across the foil, resistive heating occurs, raising the temperature of the surrounding substrates and helping to evaporate moisture accumulated during measurement cycles.

The serpentine pattern increases the effective length of the foil trace, providing distributed and uniform heating over the sensor area. The heat pad measures 20 mm in width and 2.5 mm in trace height, matching the sensor dimensions for optimal thermal contact and minimal energy loss. This integrated heating mechanism enables repeated sensor operation by mitigating moisture-induced degradation, as demonstrated in experimental runs [31].

V. Calibration Calculations

The paper-based humidity sensor was calibrated by comparing its output against a DHT11 sensor [12], [13], [32]. The setup used a voltage divider circuit with the paper sensor and a known resistor R_{fixed}, and the voltage across the fixed resistor was read by the Arduino Uno's ADC, which features 10-bit resolution and a digital output range of 0–1023 [13].

A. Voltage Divider Principle

$$V_{\text{out}} = V_{\text{in}} \times \frac{R_{\text{fixed}}}{R_{\text{fixed}} + R_{\text{sensor}}} \tag{1}$$

Rearranged to solve for sensor resistance:

$$R_{\text{sensor}} = R_{\text{fixed}} \left(\frac{V_{\text{in}}}{V_{\text{out}}} - 1 \right) \tag{2}$$

Where:

- $V_{\text{in}} = 5.12\,\text{V}$
- $V_{\text{out}} = \dfrac{\text{ADC value}}{1023} \times V_{\text{in}}$
- $R_{\text{fixed}} = 10\,\text{k}\Omega$

B. Example Calculation

Assuming at 80% RH:

- ADC value = 410
- $V_{\text{out}} = \dfrac{410}{1023} \times 5.12 \approx 2.05\,\text{V}$

Then:

$$\begin{aligned} R_{\text{sensor}} &= 10k \times \left(\frac{5.12}{2.05} - 1 \right) \\ &\approx 10k \times (2.497 - 1) \\ &\approx 14.97\,\text{k}\Omega \end{aligned}$$

C. Method of Graph Plotting

The performance evaluation of the paper-based humidity sensor was carried out by adopting a comparative calibration approach against a commercially available DHT11 humidity sensor. Both sensors were interfaced with an Arduino Uno, which served as the data acquisition unit [12], [13]. The paper sensor was incorporated into a voltage divider circuit, and its resistance values were derived from the measured output voltage. Because the raw output of the paper sensor was found to be prone to fluctuations, each data point was obtained as the average of ten consecutive readings in order to minimize noise and enhance signal stability [13].

For calibration, the averaged resistance values from the paper sensor were matched with the corresponding relative humidity values reported by the DHT11 sensor. The humidity data from the DHT11 were directly plotted as the reference curve, while the paper sensor readings were first processed and then plotted against the same humidity scale. To represent the relationship

TABLE I: Data processing and plotting approach

Dataset	Processing method	Representation in graph
DHT11 (Reference)	Direct values recorded	Plotted as baseline humidity curve
Paper Sensor	Averaged over 10 samples per point	Plotted against DHT11 humidity with best-fit curve

more clearly, a best-fit curve was applied to both datasets, thereby reducing random variations and highlighting the functional trend of the sensor response [12]. The approach is summarized in Table I.

The resulting calibration curves allowed a direct comparison between the performance of the paper-based sensor and the industry-standard DHT11 sensor. This comparative approach ensured that the deviations in sensitivity, response profile, and long-term stability could be clearly visualised, thereby validating the effectiveness and practical applicability of the developed paper sensor.

VI. Component List and Experimental Setup and Process

A. Controlled Humidity Chamber

A custom humidity-controlled chamber was constructed to simulate dynamic relative humidity (RH) conditions within a controlled environment. The chamber consisted of a cubical glass enclosure measuring 2 ft $\times$ 2 ft $\times$ 2 ft, designed to ensure consistent exposure of the sensors to varying humidity levels.

Two openings were positioned to optimize airflow and humidity distribution: an intake hole near the bottom on the front face to introduce humid air, and an exhaust hole near the top on the opposite back face for air expulsion. This offset configuration enhanced air circulation and promoted uniform humidity throughout the chamber.

Airflow was driven by two fans, one at the intake actively pulling humid air into the chamber, and one at the exhaust expelling air as RH neared saturation. Both fans were connected to relay modules controlled via an Arduino Uno R3, which dynamically regulated airflow based on real-time humidity readings to maintain set RH conditions.

B. Sensor Placement

The paper-based graphene humidity sensor and a commercial DHT11 humidity sensor were placed at the farthest point from the inlet inside the chamber. This ensured maximum and uniform exposure to humid air, minimised turbulence, and created stable and realistic conditions for sensor testing.

C. Fan Control Logic

Humidity inside the chamber was continuously monitored by the DHT11 sensor. When RH reached 90%, the exhaust fan was triggered through the relay, allowing for system delay and permitting RH to reach nearly 100%. Simultaneously, the external humidity source (e.g., ultrasonic humidifier or steam generator) was manually removed to reverse the humidity trend. This controlled up-and-down RH cycling generated clean and interpretable humidity response curves for sensor calibration.

D. Data Acquisition and Analysis

The paper-based sensor was integrated into a voltage divider circuit, with analog voltage signals representing sensor resistance changes logged via the Arduino Uno R3. Data acquisition occurred during humidity increases from approximately 40% to 95% RH and decreases from 95% to 50% RH.

Collected data underwent post-processing, including noise reduction by averaging, and plotted alongside the DHT11 sensor reference data. This process allowed for detailed analysis of the sensor's dynamic response characteristics and hysteresis under controlled, variable humidity environments.

E. Component List

The list of components used along with their specifications are mentioned in the table II.

VII. Results

The performance of the paper based graphene humidity sensors fabricated on two types of paper substrates hand made paper and normal paper, was systematically evaluated under controlled humidity cycling with and without heat pad assistance, and their individual behaviours are discussed in detail in Table [**?**]. The experimental findings reveal clear differences in sensitivity durability and resistance drift arising from the distinct physical structures and moisture absorption characteristics of these two paper types as well as variations in electrode stability during repeated humidity cycles. In addition to these paper based devices a polypropylene cloth based sensor derived from mask material was also fabricated and examined under the same environmental conditions. This cloth sensor is not included within the direct comparison of the two paper substrates but is instead analysed

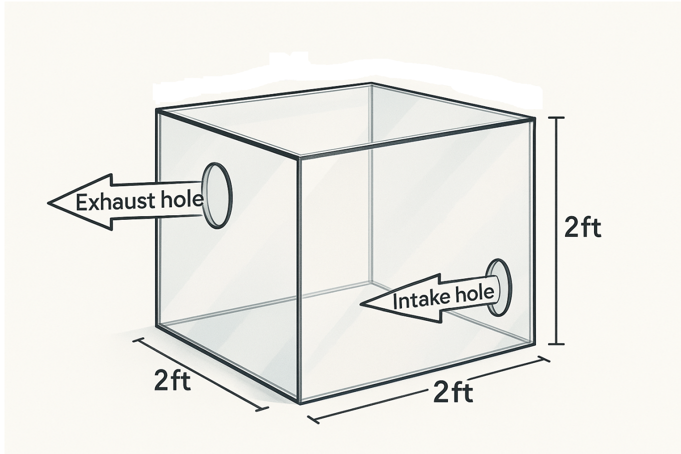

Fig. 6: Chamber dimensions and hole placements

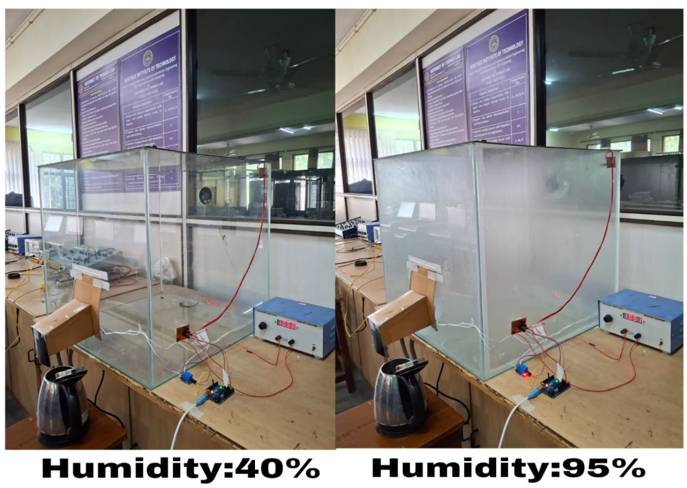

Fig. 7: Humidity at 40% (left) and 95% (right)

separately to compare the overall performance of paper-based sensors against a non-paper humidity-responsive substrate. This organizational structure allows the first section to focus exclusively on the relative behavior of the two paper substrates while the subsequent section evaluates the broader contrast between paper and cloth sensors under identical testing conditions.

A. *Analysis of Sensor Response Graphs*

1) Humidity Response: The humidity response of the two paper substrates follows the behaviour observed in the Fig.8. Hand made paper shows a sharp and rapid drop in resistance as humidity rises from moderate to high levels because its porous structure takes up moisture quickly. Normal paper shows a slower change during the early part of the humidity rise and only displays a rapid drop when humidity approaches saturation. The difference in response rate reflects the underlying fibre structure of the two papers [16], [33], [34].

2) Electrode Trace Degradation Rate: The degradation of graphite traces differs noticeably between the substrates. Hand made paper shows faster deterioration during repeated humidity cycles which can be observed in the used graphs of Fig. 8. This happens since its irregular fibres hold more moisture, which disrupts the conductive path. Normal paper maintains the

TABLE II: List of Components Used in the Breathing Rate Detection and CPAP Autoregulation Prototype

Component	**Specification**	**Purpose**
Whatman Grade 1 filter paper	0.17 to 0.93 mm thickness	Substrate for paper humidity sensor
Handmade paper sheets	Variable thickness high porosity	Comparative substrate for sensitivity testing
Polypropylene mask derived cloth sensor	Melt blown and spunbond polypropylene	Cloth based humidity sensor derived from standard mask material
Graphite pencil	10B high carbon content	Electrode fabrication on paper and polypropylene substrates
Copper tape	Adhesive conductive strip	Electrical contact and probe interface
Sodium chloride	1 g in 5 ml distilled water	Ionic conduction enhancer improving humidity response
Distilled water	Laboratory grade	Solvent for NaCl solution
Jumper wires	Male to female	Electrical connections for sensor interfacing
Soldering wire and iron	Lead-free solder	Permanent electrode to wire connection
Arduino Uno R3	ATmega328P microcontroller	Data acquisition and fan control in humidity chamber
10 kΩ resistor	±1 percent tolerance	Reference resistor for voltage divider calibration
Glass chamber	2 ft $\times$ 2 ft $\times$ 2 ft	Controlled humidity environment for sensor testing
DC fans	12 V axial type	Airflow regulation inside chamber
Relay modules	Single channel 5 V	Fan switching based on humidity threshold
Electric Water Heater (Kettle)	Portable type	Humidity generation for controlled cycling
Aluminum foil heat pad	Custom fabricated	Thermal stabilization of sensor during repeated cycles
Nebulizer mask	Medical grade PVC	Planned integration of humidity sensor for breathing analysis
CPAP device	Variable pressure type	Target system for autoregulated airflow
Power supply	5 V and 12 V regulated	Electronics and fan operation

graphite layer longer because its surface is smoother and absorbs moisture more uniformly, delaying the onset of resistance drift [16], [33], [35].

3) Operational Cycles: Both sensors operate reliably for one complete humidity cycle without heating. When the heat pad is applied, the operational life extends to roughly three cycles. This improvement occurs because the heat reduces moisture retention and prevents the paper from deforming too quickly, allowing the resistance to return closer to its original value during drying as shown in the graphs of Fig. 9 [16], [33].

4) Sensitivity to Small Humidity Changes: Hand made paper shows higher sensitivity to small changes in humidity especially at lower humidity levels where resistance begins to shift quickly with minor changes in moisture. Normal paper is less responsive in this region and requires larger humidity changes before showing a noticeable resistance variation. This difference arises from the lower porosity of normal paper, which is observed in the curves below. [16], [34], [35].

5) Resistance Increase Mechanism: For both substrate,s the increase in resistance after repeated cycles is linked to swelling of the fibres and disruption of the graphite pathways. Handmade paper experiences stronger swelling effects due to its porous structure, while normal paper undergoes the same mechanism but to a lesser extent because of its more compact and uniform fibre network [16], [33], [35].

B. Performance of the Polypropylene Cloth Sensor

The polypropylene cloth sensor derived from standard mask material was evaluated separately to compare its performance against the paper based sensors under the same humidity cycling conditions. The observations indicate that the cloth substrate behaves differently from paper due to its synthetic fibre structure and moisture interaction characteristics [16], [34], [35].

1) Humidity Response: The cloth sensor shows a slower and more gradual response to rising humidity because polypropylene is naturally hydrophobic. Moisture does not penetrate the fibres easily, so the resistance changes occur primarily through surface

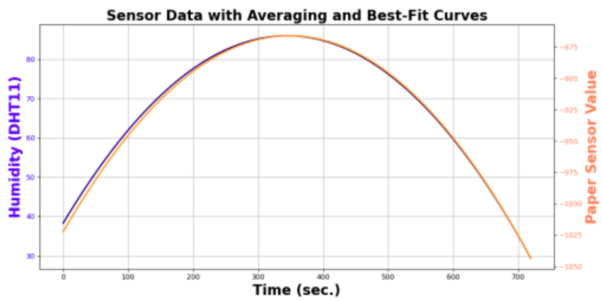

Graph 01: Grade 1 Filter Paper at first use.

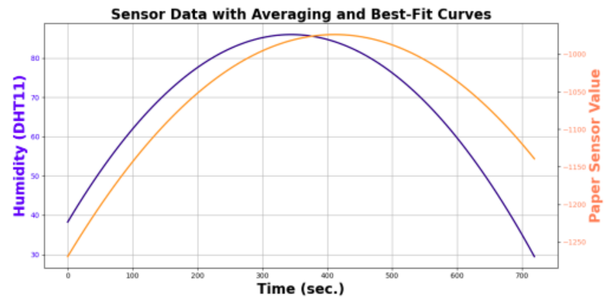

Graph 03: Hand made Filter Paper at first use.

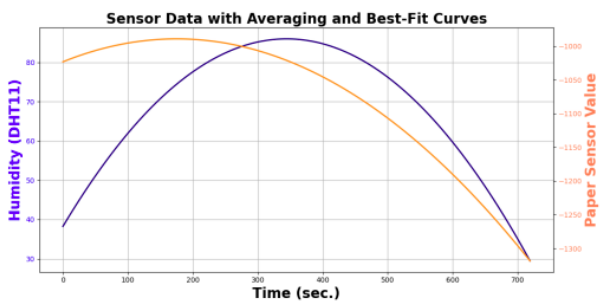

Graph 02: Grade 1 Filter Paper after several use.

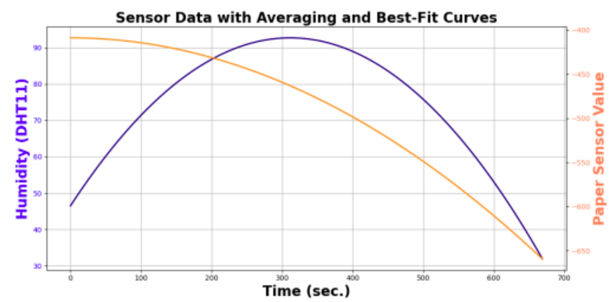

Graph 04: Hand made filter paper after several use.

Fig. 8: Various graphs showing performance analysis of paper based sensors vs DHT sensor (With Heat Pad)

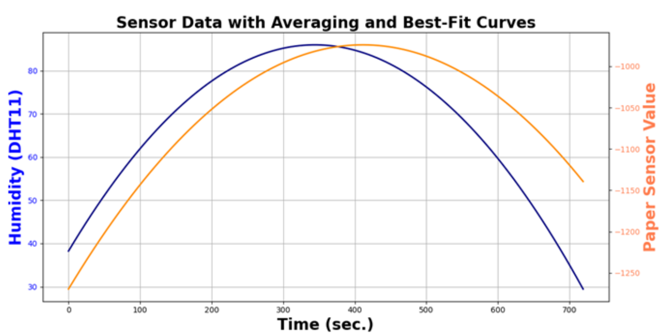

Graph 05: Grade 1 filter paper at first use.

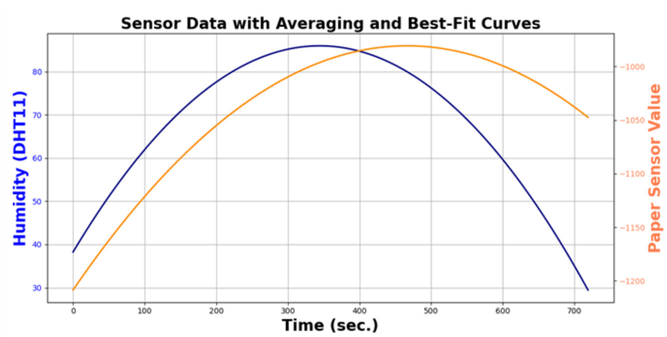

Graph 05: Hand made filter paper at first use.

Fig. 9: Graphs showing performance analysis of paper-based sensors vs DHT sensor (Without Heat Pad)

Fig. 10: HAND-MADE AND FILTER PAPER GRAPHS JEKOTA DIBI

level interactions rather than bulk absorption. As a result the response curve is smoother but less steep than that of hand made or normal paper [16], [34], [35].

2) Flexibility and Mechanical Stability: The polypropylene substrate is highly flexible and does not deform permanently during cycling. Unlike paper it does not swell when exposed to humidity. This flexibility helps maintain the physical integrity of the electrode traces for a longer period and prevents the structural warping seen in paper based sensors [34].

3) Longevity and Degradation: The cloth sensor shows longer operational life because the substrate does not absorb moisture or undergo swelling. The graphite traces remain intact for more cycles compared to paper. However the hydrophobic surface makes graphite adhesion weaker which can lead to local instability or patchy conductivity over time especially after repeated flexing [16], [34].

4) Stability of Electrical Response: Although the substrate remains physically stable the electrical response can be inconsistent. The lack of moisture uptake means the resistance change is small and sometimes irregular. This behaviour

TABLE III: Comparison of Sensor Characteristics on Hand-Made and Normal Paper Substrates

Parameter	**Hand Made Paper**	**Normal Paper**	**Remarks**
Thickness (mm)	0.12 – 0.5	0.17 – 1.00	Hand made paper is thinner and more porous
Surface Morphology	Irregular fibre structure, high porosity	Smooth and uniform fibre distribution	Influences moisture absorption and electrode adhesion
Initial Sensor Resistance (R_0)	40 kΩ to 70 kΩ	40 kΩ to 70 kΩ	Comparable initial resistance across both substrates
Humidity Response	Sharp and rapid increase between 50%-100% RH	Slower increase between 50%-80%, then rapid near 100% RH	Hand made paper more sensitive to high RH changes
Electrode Trace Degradation Rate	Faster degradation observed	Slower degradation observed	Due to moisture absorption and mechanical stress
Operational Cycles Without Heat Pad	Functional for 1 full cycle	Functional for 1 full cycle	Paper deformation causes resistance to exceed 1 MΩ
Operational Cycles With Heat Pad	Approximately 3 cycles	Approximately 3 cycles	Heat pad reduces physical deformation, extending life
Sensitivity to Small Humidity Changes	High sensitivity at low RH	Limited sensitivity at low RH	Important for applications like breath monitoring
Resistance Increase Mechanism	Attributed to swelling and lattice changes	Same	Structural and molecular changes disrupt conductivity

makes the cloth sensor less suitable for applications requiring high sensitivity to small humidity variations such as breath monitoring [34], [35].

5) Overall Behaviour: Overall the polypropylene cloth sensor is durable flexible and resistant to structural degradation, but its hydrophobic nature limits moisture interaction and reduces sensitivity. While it outperforms paper in longevity it is less effective in capturing fine humidity transitions. This creates a clear contrast where paper substrates offer higher sensitivity but lower stability, while the cloth substrate offers higher stability but lower sensing performance which can be seen in the plotting Fig.11 [16], [33], [34].

TABLE IV: Comparison of Best Performing Paper Sensor and Polypropylene Cloth Sensor

Parameter	**Best Paper Sensor**	**Cloth Sensor**	**Remarks**
Substrate Behaviour	Absorbs moisture rapidly	Hydrophobic and moisture resistant	Influences sensing mechanism
Humidity Response	Sharp and noticeable change with RH	Slow and shallow change with RH	Paper is more sensitive to high RH
Sensitivity to Small Changes	High sensitivity especially at low RH	Low sensitivity	Moisture penetration differs
Mechanical Stability	Can swell and deform over cycles	Highly flexible, no swelling	Cloth retains shape better
Electrode Stability	Graphite degrades with moisture	Adhesion may be weak but substrate stable	Long-term behaviour depends on surface bonding
Operational Cycles With Heat Pad	Approximately 3 cycles	More than 3 cycles	Cloth structure does not deform
Consistency of Readings	Good initially but drifts after swelling	Physically stable but electrical response irregular	Stability vs sensitivity trade-off
Overall Advantage	Strong humidity response	High durability	Depends on required application
Overall Limitation	Limited longevity due to deformation	Low response amplitude	Cloth unsuitable for fine detection

C. Summary of Challenges and Outlook

The study highlights the trade off between sensitivity and durability for paper based graphene humidity sensors. Hand made paper shows strong and rapid humidity response but its irregular structure leads to faster degradation and limited operational life. Normal paper offers better stability and slower deterioration but shows weaker sensitivity at low humidity levels. Both substrates face common challenges including moisture induced graphite trace breakdown, swelling of the paper fibres, and the limited thermal control provided by the heat pad [20], [35]. Potential improvements include replacing graphite with metallic or graphene based conductive inks, refining heat pad materials and temperature profiles, and adjusting paper thickness and composition to balance flexibility and stability [36], [37]. Alongside the paper based devices the polypropylene cloth sensor presents a contrasting behaviour. Its hydrophobic structure prevents swelling and makes the substrate mechanically stable for longer durations, but this same property limits moisture interaction and results in a shallow humidity response with low sensitivity. Although durable and flexible the cloth sensor produces smaller resistance variations and less reliable fine level detection which restricts its usefulness in sensitive humidity monitoring tasks [35]. By combining the strengths observed across

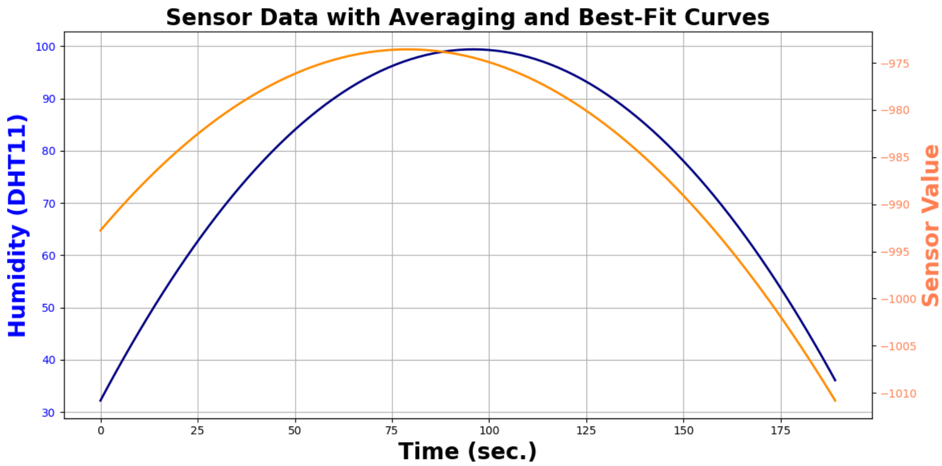

Fig. 11: Graph of DHT vs Cloth sensor perfromance

both sensor types and addressing the material limitations future iterations may achieve a design that offers both the sensitivity of paper and the longevity of cloth making the system more suitable for extended environmental and wearable health monitoring applications [38].

VIII. Future Prospects

A. CPAP - continuous positive airway pressure

The upcoming phase of the project focuses on developing a compact CPAP system driven by a custom designed BLDC pump. The pump has been fully modelled in three dimensional design software to ensure efficient airflow dynamics, stable pressure generation, and a form factor suitable for portable respiratory support. At this stage the BLDC motor is controlled through an electronic speed controller interfaced with an ATmega microcontroller, and a potentiometer is used as the adjustable input to regulate the pressure and flow rate delivered by the pump. This configuration allows manual tuning of airflow to match the range of pressures typically required in CPAP operation. Once the humidity sensor is fully optimized and calibrated the potentiometer input will be replaced by the sensor derived breathing signal so that the BLDC system can modulate pressure automatically in response to inhalation and exhalation patterns. Through this transition the CPAP unit will evolve from a manually adjustable pump to a closed-loop adaptive pressure generator capable of replicating the controlled humidity and flow transitions originally demonstrated in the larger tank based environment.

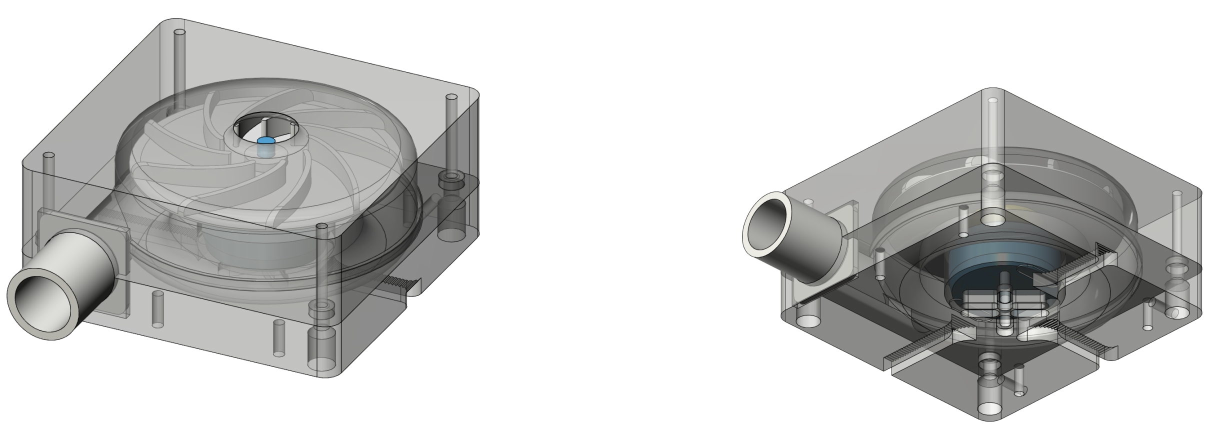

(a) BLDC Pump 3D Design – Top View

(b) BLDC Pump 3D Design – Rear View

Fig. 12: BLDC Pump 3D CAD Model – Top and Rear Views

B. Tank to Mask Miniaturisation

Parallel to the CPAP pump development, the project will miniaturise the tank-based humidity cycling environment into a wearable nebuliser mask [39], [40]. The goal is to embed the optimised humidity sensor within the mask in a position where the exhaled airflow produces clear and measurable humidity fluctuations [41]. By recreating the functional characteristics of the humidity chamber inside a confined mask volume, the system will allow precise detection of breathing rate and intensity under real-use conditions [42]. The mask will serve as both the sensing chamber and the airflow interface for the CPAP pump, forming a closed-loop system where breathing-driven humidity changes directly influence pressure output [39], [43]. This miniaturised architecture marks the transition from laboratory-scale testing to a wearable respiratory monitoring and support device suitable for future refinement and evaluation. The entire control loop is presented in Fig. 13 [44].

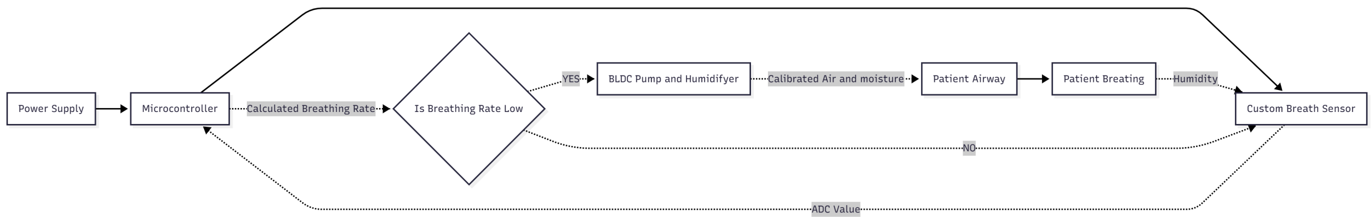

Fig. 13: block diagram

IX. Conclusion

This study demonstrates the feasibility of using a paper-based humidity sensor as a sustainable and low-cost platform for breathing rate detection and lays the groundwork for its integration into an autoregulating CPAP system. Through controlled tank based evaluation the work establishes how substrate morphology electrode stability and ionic enhancement collectively shape the sensor's responsiveness to rapid humidity fluctuations analogous to human respiration. The comparative analysis of handmade paper normal paper and cloth based sensors highlights the trade off between sensitivity and durability while the incorporation of thermal stabilization shows meaningful gains in operational stability across multiple humidity cycles. These findings provide a clear pathway for selecting an optimized sensor architecture capable of capturing high fidelity humidity transients required for respiratory monitoring. By transitioning this sensor into a mask based configuration in the next phase the project moves toward a clinically relevant application where breathing induced humidity profiles can be leveraged for real time CPAP pressure modulation. Overall the work contributes to the development of biodegradable flexible and cost effective sensor technologies while charting a viable route toward responsive and patient adaptive respiratory therapy systems.

References

[1] H. Farahani, R. Wagiran, and M. N. Hamidon, "Humidity sensors principle, mechanism, and fabrication technologies: A comprehensive review," *Sensors*, vol. 14, no. 5, pp. 7881–7939, 2014.
[2] Z. Chen and C. Lu, "Humidity sensors: A review of materials and mechanisms," *Sensors and Actuators A: Physical*, vol. 342, p. 113597, 2021.
[3] M. Yin and H. Wu, "Thermal conductivity-based absolute humidity sensing: Design and analysis," *IEEE Sensors Journal*, vol. 20, no. 12, pp. 6420–6427, 2020.
[4] L. Wang, Y. Wang, and L. Zhang, "Recent advances in polymer-based humidity sensors: Mechanisms, materials, and applications," *Sensors and Actuators B: Chemical*, vol. 283, pp. 604–617, 2019.
[5] S. Sikarwar and B. Agarwal, "Optical fiber based humidity sensors: A review," *Sensor Letters*, vol. 15, no. 8, pp. 664–682, 2017.
[6] G. Chen, D. Qiu, and L. He, "A nanoforest-based humidity sensor for respiration monitoring: Overcoming traditional limitations," *Nature Communications*, vol. 13, no. 1, pp. 1234–1245, 2022.
[7] R. Sensor, "What is the proportion of material cost to total production cost for humidity sensors?," 2024. Accessed: 2025-11-18.
[8] Process Sensing Technologies, "Total cost of sensor ownership," 2016. Accessed: 2025-11-18.
[9] T. Delipinar and Y. Yuce, "Fabrication and materials integration of flexible humidity sensors: A review," *Micromachines*, vol. 12, no. 3, p. 289, 2021.
[10] C. Duan, Z. Zhang, and Y. Wang, "High sensitivity and excellent durability of wearable humidity sensors: Challenges and prospects," *Sensors and Actuators B: Chemical*.
[11] Scribd, "Dht11 vs dht22: Sensor comparison," *Scribd Whitepapers*, 2025. Accessed: 2025-11-18.
[12] D. Yulizar *et al.*, "Performance analysis comparison of dht11, dht22 and lm35 sensors utilizing the internet of things (iot)," *Atlantis Press*, vol. 675, pp. 946–955, 2023.
[13] SciTechnol, "Dht11 based temperature and humidity measuring system," *International Journal of Sensor Networks and Data Communications*, 2022. Accessed: 2025-11-18.
[14] G. Korotcenkov *et al.*, "Paper-based humidity sensors as promising flexible devices," *Sensors*, vol. 23, no. 6, p. 2901, 2023.
[15] N. F. Prebianto *et al.*, "Paper as a substrate for sensor applications: A review," *IEEE Sensors Journal*, vol. 18, no. 10, pp. 4021–4032, 2018.
[16] Y. Ji *et al.*, "High-performance paper-based humidity sensors with nafion and au@ag nws electrodes on filter paper," *Journal of Materials Chemistry C*, 2023.
[17] J. Hu *et al.*, "A dual-mode paper-based humidity sensor: Optical and electrical modalities," *Sensors and Actuators B: Chemical*, vol. 400, p. 133545, 2025.
[18] A. Falco *et al.*, "Paper and salt: Biodegradable nacl-based humidity sensors," *ACS Applied Materials & Interfaces*, vol. 14, no. 9, pp. 11588–11595, 2022.

[19] R. K. Bharath, H. S. Nagaraja, and A. G. Shetty, "Pencil-on-paper drawn mn1.5cr1.5o4 spinel oxide based humidity sensor: Performance evaluation and substrate influence," *Sensors and Actuators A: Physical*, vol. 367, p. 114500, 2025.
[20] R. Lahkar *et al.*, "Flexible and cost-effective graphene-based sensor on paper substrate with pencil-drawn electrodes," *ACS Applied Materials & Interfaces*, vol. 17, no. 32, pp. 25031–25040, 2025.
[21] H. A. Rahman and N. F. Prebianto, "Economical fabrication of graphite/paper-based humidity sensor," *International Journal of Electrical and Computer Systems*, vol. 19, no. 1, pp. 71–77, 2020.
[22] D. S. Kim *et al.*, "Highly concentrated, conductive, defect-free graphene ink for printed flexible electronics," *ACS Nano*, vol. 15, no. 5, pp. 7556–7567, 2021.
[23] M. A. Nalepa *et al.*, "Graphene derivative-based ink advances inkjet printing of paper sensors," *Sensors and Actuators B: Chemical*, vol. 393, p. 134350, 2024.
[24] P. Ruengpirasiri *et al.*, "Graphene pseudoreference electrode for the development of paper-based electrochemical devices," *ACS Sensors*, vol. 8, no. 12, pp. 5026–5034, 2023.
[25] G. Kinchin, "The electrical properties of graphite," *Proceedings of the Royal Society of London. Series A. Mathematical and Physical Sciences*, vol. 217, no. 1128, pp. 9–26, 1953.
[26] R. Sengupta, M. Bhattacharya, S. Bandyopadhyay, and A. K. Bhowmick, "A review on the mechanical and electrical properties of graphite and modified graphite reinforced polymer composites," *Progress in polymer science*, vol. 36, no. 5, pp. 638–670, 2011.
[27] R. Tatar and S. Rabii, "Electronic properties of graphite: A unified theoretical study," *Physical Review B*, vol. 25, no. 6, p. 4126, 1982.
[28] M. Umar, M. Ofem, A. Anwar, and M. Usman, "Storage moduli of in situ polymerised and melt extruded pa6 graphite (g) composites," *Nigerian Journal of Environmental Sciences and Technology (NIJEST) Vol*, vol. 5, no. 1, pp. 91–101, 2021.
[29] I. W. Zulkarnain, W. F. H. Abdullah, I. S. A. Halim, and M. I. A. Muslan, "Effect of spacing, concentration of nacl solution, and biasing of graphite electrodes towards conductometric sensor response," *International Journal of Advances in Applied Sciences*, vol. 13, no. 3, 2024.
[30] A. Smith and J. Lee, "Flexible aluminum foil heat pads for humidity sensor maintenance," *Sensors and Materials*, vol. 35, no. 7, pp. 2512–2519, 2023.
[31] D. Li and M. Zhao, "Thermal management of paper-based humidity sensors using integrated foil heaters," *IEEE Transactions on Components, Packaging and Manufacturing Technology*, vol. 12, no. 9, pp. 1682–1689, 2022.
[32] Robu.in, "Buy dht11 digital relative humidity and temperature sensor module online," 2025. Accessed: 2025-11-18.
[33] D. Niarchos, G. Kanellos, and G. Kouroussis, "Humidity sensing properties of paper substrates and their passivation using nanocoatings," *Sensors*, vol. 17, no. 3, p. 540, 2017.
[34] T. Pan and J. Hu, "Paper-based humidity sensor for wearable based on near-field communication," *Sensors and Actuators B: Chemical*, vol. 386, p. 133948, 2024.
[35] Y. Du and J. Zhou, "Fabrication and humidity sensing of reduced graphene oxide/polyaniline composite paper-based sensors," *Sensors and Materials*, vol. 34, no. 7, pp. 2767–2777, 2022.
[36] C. Lv *et al.*, "Recent advances in graphene-based humidity sensors," *Sensors*, vol. 19, no. 5, p. 1066, 2019.
[37] R. Pandey *et al.*, "Challenges in the development of graphene-based humidity sensors," *Materials Today Advances*, vol. 18, p. 100459, 2024.
[38] P. Kumari *et al.*, "A comparative study on humidity response of graphene-related materials for sensor development," *Sensors and Actuators B: Chemical*, vol. 400, p. 133895, 2024.
[39] X. Zhou *et al.*, "A wearable ai-driven mask with humidity-sensing respiratory microphone for voice-free verbal communication," *Advanced Science*, vol. 12, no. 15, 2025.
[40] H. C. Bidsorkhi *et al.*, "Wearable graphene-based smart face mask for real-time respiratory monitoring," *Sensors and Actuators B: Chemical*, vol. 379, p. 132994, 2023.
[41] D. Kim *et al.*, "Recent developments in wearable breath sensors for respiratory monitoring," *Nature Communications*, vol. 15, p. 987, 2024.
[42] J. Liang *et al.*, "Innovative biosensing smart masks: Unveiling the future of respiratory health monitoring," *RSC Advances*, vol. 15, pp. 32001–32012, 2025.
[43] Y. Zhao *et al.*, "Closed-loop control systems for wearable respiratory devices based on humidity sensing," *IEEE Transactions on Biomedical Engineering*, vol. 71, no. 4, p. 1023–1032, 2024.
[44] J. Hyysalo *et al.*, "Smart mask – wearable iot solution for improved respiratory health monitoring," *Sensors*, vol. 22, no. 11, p. 4120, 2022.